2018

Effect Of Material Orientation On The Impact Response Of Graded Cellular Materials

Abigail Wohlford
University of South Carolina

Effect of Material Orientation on the Impact Response of Graded Cellular Materials

by

Abigail Wohlford

Bachelor of Science
University of South Carolina, 2016

Submitted in Partial Fulfillment of the Requirements

For the Degree of Master of Science in

Mechanical Engineering

College of Engineering and Computing

University of South Carolina

2018

Accepted by:

Addis Kidane, Director of Thesis

Michael A. Sutton, Reader

Cheryl L. Addy, Vice Provost and Dean of the Graduate School

ACKNOWLEDGEMENTS

First and foremost, I would like to extend my sincerest gratitude to my advisor Dr. Addis Kidane who first got my interested in doing research during my undergraduate studies and pushed me to be my best. He believed in me when I had doubts and he helped guide me through my graduate career. I'm grateful to have had the privilege of learning from the esteemed Dr. Michael Sutton. Acquiring my Master's Degree would not have been possible without my officemate, Addis Tessema. He showed me the ropes of what it means to be a researcher and progress to the next level of academia. I also want to thank Suraj Ravindran whose talent in experimental mechanics is unmatched. This work is an extension of the research done by Behrad Koohbor who gave me incredible guidance and helped point me in the right direction. I want to show my appreciation to Ali Fahem for helping me learn the different experimental procedures. Many thanks to Vijendra Gupta and Dennis Miller for their assistance running experiments. I will forever cherish the opportunity I had to work alongside these intellectual minds. Lastly, I would like to acknowledge the Army Research Office for their financial support in this project.

ABSTRACT

In this study, the effect of layer stacking on the energy absorption characteristics of density-graded cellular polymers subjected to high velocity impact is investigated experimentally. The focus in the present work is to characterize the constitutive response and deformation mechanisms of these Functionally Graded Foam Materials (FGFM) using full-field measurements. Uniform foam Quasi-static and dynamic testing of uniform foam specimens are completed for each nominal density used in the layered foam samples. The low strain-rate experiments are performed in order to determine the mechanical properties of foam specimens. The high-rate experiments for homogenous foam specimens were completed to further characterize the constitutive response and also to provide baseline data for comparison to the response of FGM specimens. High rate loading experiments are performed using Split Hopkinson Pressure Bar (SHPB) combined with ultra-high-speed imaging to measure in-situ deformations and observe the formation and propagation of elastic and inelastic stress waves during impact. The FGM specimens were fabricated in-house by bonding different bulk density polymeric foam layers in different stacking arrangements. The effect of the orientation of the discrete layers on the dynamic response is quantified using high speed imaging with digital image correlation (DIC). The challenges with dynamic equilibrium due to low mechanical impedance of soft materials are carefully considered. The effects of inertia and material compressibility are included in analysis. The approach uses DIC to gather the full-field data which is used to measure the acceleration and density, later used to estimate the

stress gradients developed in the material. The temporal and spatial distributions of the inertia stress are superimposed with the boundary stress measured from the transmitted signal to satisfy the equation of dynamic stress equilibrium. The local and global responses are both examined in order to assess the overall performance of each gradient sequence. The average stress-strain curves obtained are then used to find the total energy absorbed during loading. Since the desired final goal is to be able to optimize this graded cushioning structure for any specific situation, the "best" arrangement of the FGM system is defined to be the layered system that has the highest energy absorption based on the model being used to characterize response. Recommendations for the extension of this work will be made at the end.

TABLE OF CONTENTS

LIST OF FIGURES

LIST OF ABBREVIATIONS

ASTM ..... American Section of the International Association for Testing Materials

DIC..... Digital Image Correlation

FGFM..... Functionally Graded Foam Material

FGM..... Functionally Graded Material

SHPB..... Split Hopkinson Pressure Bar

CHAPTER 1

INTRODUCTION

1.1 OVERVIEW OF FOAM & FUNCTIONALLY GRADED MATERIALS

Polymeric foams are widely used due to their relatively high specific strength, low density, and superior energy absorption characteristics. They have become increasingly relevant because of their light structural weight, ability to be molded into complex geometries, and their capability to reduce injury or damage caused by an explosion[1]. The ideal energy dissipation of these soft materials is a result of the porous structure of these foams. The deformation mechanisms at the cellular scale are cell wall bending leading up to wall buckling or fracture after yielding; this process is typically how energy is absorbed in such systems[2]. Owing to these desirable characteristics, foam materials are commonly used as cushioning or protective structures in a variety of industries including automotive, aerospace, marine vessels, and consumer product packaging for transport. Since structural foams can be soft and flexible, or relatively stiff, but still deformable, such systems can be especially effective due to the dissipation of energy by permanent deformation and progressive crushing of its microstructure. In addition to typical quasi-static applications, foam systems have great potential in dynamic loading applications including high-velocity impact loading. Though foams have been shown to be good energy absorbers, the ability to predict their dynamic response is complicated by their very high strain-rate dependency, presence of inertial effects, and the change in foam density that occurs during crushing. These effects result in highly

nonlinear mechanical response at a variety of scales in such cellular materials. Here, the continuum scale response is directly linked to the mechanisms of deformation occurring at the level of an individual foam cell, so that the macroscopic mechanical properties of foam are correlated with the base material and the complex microstructure[3].

It is well known that the strength and energy absorption are highly sensitive to the relative density of the polymeric foam. Defining relative density, ρ^*/ρ_s, as the ratio between the density of the cellular material, ρ^*, and the parent solid material from which the cell walls are made,ρ_s, as the relative density increases, the cell walls thicken and the pore space diminishes; this intuitively indicates that the "strength" of the material will increase.

Since the main requirements for an energy-absorbing structure is to dissipate the kinetic energy generated from an impact while ensuring the maximum resisting force is below a certain limit, it is intuitively clear that the cell size and selection of the parent material must be optimized. The foam structure will have a much smaller max force than the parent (matrix) material of equal volume for the same amount of energy dissipated[4]. These porous materials have a low volume fraction of the parent material, which allows for large degrees of plastic crushing to occur at a constant plateau stress until the densification strain is reached[5]. The main difference between foam and a solid dense material is the big volume change; there is less lateral spreading, instead the cells are simply collapsing. The complex cellular microstructure allows for large deformation to occur at a constant nominal stress, so large amounts of energy can be absorbed without generating high stress. Higher density foams show higher strength compared to lower density foams but possess lower densification strain. Thus, with homogeneous foam there

occurs a compromise between energy absorption, strength, and weight with foams of different densities.

In order to possess a high level of all these sought-after characteristics, the concept of graded foam is introduced. Functionally Graded Materials are in the family of advanced engineering composites designed for a specific function or application. The basic idea is to take advantage of the unique properties of the individual components and combine them to tailor a single enhanced structure. FGMs have either a gradual or a stepwise change in material properties along a specific direction. A graded material has better designability and will at the very least have an equal outcome, but will more likely outperform its corresponding uniform material[6]. FGMs originally gained a lot of attention as metal-ceramic composites to have a gradually changing thermal expansion coefficient. FGMs were not invented by engineers though, they appear in nature such as bones or plants, where the cellular structures vary in thickness or size. FGM's are advanced multifunctional materials with spatial gradation in composition, i.e. the mechanical properties.

As noted by Minoo Naebe [7], "The ability to understand and manipulate materials has been fundamental to our technical development over time.". Many researchers have taken an interest in the mechanical response of FGMs concerning the load response to dynamic loading, and the energy absorbing characteristics of cellular graded structures. With functionally graded foams, the desire is to diminish the peak acceleration generated from impact in order to mitigate the stress wave[5]. The stepwise crushing from the lowest density to the highest allows the stress to gradually dampen out.

For the example of a helmet liner, the density gradient could reduce the severity of the injury induced in the person being protected[2].

The capability to optimize a structure by gradually varying the morphology is something most any scientist would be interested in, and offers large possibilities for engineering ingenuity. The prospect of continuously graded materials has been pursued by many to have a material with specific spatial variation of structural properties. The fabrication and manufacturing techniques of continuous functionally graded materials are being developed; there are many challenges still involved in the processes. The utilization of FGMs and their multifunctional properties can reduce stress in the overall structure. The material architecture has great potential to improve structural performance and meet the many demands of advanced materials to solve a wide array of problems. Graded cellular materials are highly developed structures thanks to their evolving solid-volume fractions in the preferred material axis orientation. The continued advancements and research into Functionally graded foam materials will lead to improved light-weight energy absorbing structures for any loading condition.

1.2 OUTLINE AND OBJECTIVE

The structure of this work will comprise of different analyses of homogeneous and heterogeneous cellular materials. The mechanical characterization of uniform and graded foams is presented for various strain rates. The full-field measurements are acquired using Digital Image Correlation. First the constitutive response of the uniform foam is examined for quasi-static and dynamic loading rates. The mechanical properties for each density foam are acquired. Next the linear graded foam structure is compared with the

responses of each uniform foam. Lastly the placement of the different density layers will be rearranged to analyze the effect of the sequence of mechanical properties.

The objective of this present work is to accurately experimentally characterize dynamic response of FGFMs and optimize the gradient for energy absorption. The full-field stress is calculated by superimposing the boundary-measured stress with the calculated inertia stress. The stacking sequence of discretized layers of different bulk densities is varied to determine the ideal gradation for load bearing performance. FGFM samples are constructed and subjected to dynamic loading via SHPB to generate stress in the discretized foam samples. Based on the experimental results the effects of orientation on the response of FGM's are analyzed by observing the stress-strain response. The conclusion of these experiments will serve to improve the understanding of graded energy absorbing structures and optimize protective cushioning structures in their endless array of applications.

CHAPTER 2

LITERATURE REVIEW

Foam materials have attracted a lot of attention for many years especially when energy dissipation and low structural weight are desirable design considerations. In order to use these materials in applications and design, the mechanical response needs to be well defined for any loading condition. The quasi-static response has long well been understood and accepted and used to define these structures. However, it is not a fair assumption to make that the defined quasi-static properties can properly characterize the material in all real-life scenarios. Attributable to the many applications that involve damage protection there is a need for understanding of the response of these low-mechanical-impedance materials under high strain rate loading conditions. But the dynamic mechanical responses of these materials under such conditions are not well understood.

There are many issues that come into play with dynamic testing of polymeric foams. Soft materials possess low stiffness, yield strength, and wave speeds. Low stiffness requires highly sensitive load detection, the low strength causes significant inertia effects, and the low wave speed delays stress equilibrium. Chen[8] addressed the issues with using the Kolsky technique for soft-material characterization and offered remedies to better obtain more accurate results. The use of polymeric bars has been employed to reduce the impedance mismatch thereby improving the accuracy of the transmitted signal [9]. Liu [10] offered a solution using large diameter nylon Hopkinson

bars in conjunction with optical field measurements. Some researchers have explored the transient stress-state to investigate the initial dynamic deformation under impact. A non-parametric method was developed to be able to discount the dynamic equilibrium assumption. The technique [11] deduces the stress-strain relation at any point on the specimen using a force measurement at the specimen boundary and a displacement measurement using Digital Image Correlation. It was found that some parts of the material were strained up to 5% while the distal end wasn't strained at all. Pulse-shaping techniques have been introduced to ensure uniform deformation of low-impedance materials at high strain rates [12]. Hu analyzed the dynamic behavior of hexagonal honeycombs, another species of cellular materials ideal for energy absorption. He found that 90% of the crushing strength is attributed to inertia effects under dynamic crushing conditions. This goes to show why cellular materials possess higher crushing strength under impact loading versus quasi-static conditions [13]. There are many analyses and methods of characterization that have been proposed specifically on energy absorption of soft materials. Avalle [4]examined the energy absorption characteristics of compressive impact loading on polymeric foams using the energy-absorption diagram method.

While the examination of homogeneous foam is nothing new, the investigation of functionally graded foams is still in its early stages. Functionally graded materials first gained a lot of interest as a combination of ceramic and metals, eliminating sharp interfaces that caused severe stress localizations. Virtual FGFMs have been studied by Kiernan[14] using SHPB and the energy dissipation was found to be shaped by the gradient. He found that the propagation of the stress wave was discernibly defined by the variation in density; consequently, the damage inflicted on the object being protected

could be reduced. Finite element simulations showed that FGFMs exhibit superior characteristics over the equivalent uniform foam and that the density range plays a role in the performance of the graded foam[2]. The determination of the ideal density range is dependent on if the impact is high or low energy.

Numerical simulations require the actual physical response to authenticate the material models. Functionally graded syntactic foams were fabricated that were capable of reaching 60-75% compression without significant loss in strength[15]. The compressive strain and strength were found to be dependent on the composition of the material with strong sensitivity to the weakest layer in the structure. The functionally graded syntactic foam was found to have 200-500% increased energy absorption versus the comparable plain foam [16]. Sandwich configurations with middle-high and middle-low density distributions were analyzed with respect to their impact response. They were investigated theoretically and numerically and found to improve the energy absorption [17]. Koohbor [18] employed an analytical approach to study the effect of discrete and continuous density gradation which was validated with experimental data. The optimal gradation is contingent on the amount of deformation that would be exerted on the structure. It is apparent that the gradient effect of these materials has been carefully studied analytically and theoretically but there still lacks experimental work in the literature.

CHAPTER 3

CONSTITUTIVE RESPONSE OF UNIFORM FOAM

3.1 ABSTRACT

Cellular materials are abundantly used in commercial, industry, and military applications therefore there is a necessity for a thorough understanding of their non-linear properties and viscoelastic response. Furthermore, effective testing methods have required innovation for these unique materials. The constitutive behavior of homogeneous polymeric foam is investigated experimentally at various loading rates. Quasi-static and dynamic experiments are performed to observe the materials' response at differing strain rates. MTS and Split Hopkinson Pressure Bar (SHPB) are used along with Digital Image Correlation to perform the experiments. Polyurethane samples of five different densities were examined to observe the effect of the relative density. A non-parametric method based on force measurement at the specimen boundary and the strain field measured from DIC is implemented to identify the stress field.

3.2 INTRODUCTION

Polymeric foams are widely used in energy absorption applications across many industries. Foams make exemplary dampers due to their ability to reduce noise. They are relatively cheap and have great heat insulation along with their many other redeeming properties. Structural foams are commonly used as the core of sandwiches. There are many applications that are leading to the use of these soft materials in high rate and large deformation situations. For that purpose, there has come an increasing amount of study

into the strain rate dependency. Chen [19] modified a SHPB to perform dynamic compressive experiments on polymeric foams and found the dynamic stress levels to be twice as much as the corresponding quasi-static values. Weißenborn adapted an analytical model to predict the strain rate relationship to the stress-strain response for foams with different densities [20]. Validating the results with experimental tests it was found that there is increasing strain rate sensitivity with higher density foams.

The majority of dynamic loading methods are valid only when the stress and strain are homogeneous. But with the low impedance of foam, dynamic equilibrium is difficult to achieve. A new method using the full-field measurements of strain and inertia stress is implemented to account for the delayed stress equilibrium. The inertia stress is superimposed with the measured boundary stress from SHPB using a reconstructed general dynamic stress equilibrium equation. The mechanical properties and constitutive response are acquired for five foams of differing nominal density. The average stress-strain response of each foam will be presented since the materials do not deform uniformly. The stress-strain curve is used to calculate the energy absorbed for each material.

3.3 MATERIAL AND SPECIMEN GEOMETRY

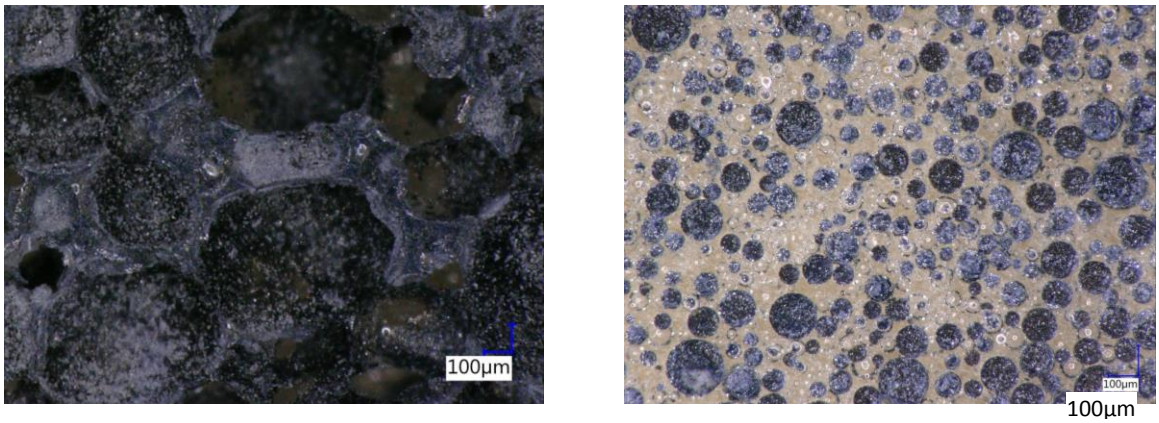

Figure 3.1. Lowest and highest density microstructure

Rigid closed cell foams are used, meaning the gas-filled pores are sealed, or isolated. The foams used for this experiment are considered "soft materials" because using the Kolsky method, a specimen having a strength less than 10 MPa presents issues associated with soft material characterization[8]. Polyurethane foams of 64 kg/m^3, 160 kg/m^3, 320 kg/m^3, 480 kg/m^3, and 640 kg/m^3 nominal densities were purchased from General Plastics, specifically the FR-7100 Aerospace grade series. So, the matrix material is the same for every sample but the pore size is varying. The difference in the microstructure is shown in Figure 3.1 for the lowest and highest density foams. Rectangular prism specimens of 25.4 x 17 x 17 mm^3 for both sets of experiments were fabricated in-house. The samples were extracted from the as-received billets supplied by General Plastics using a band saw, and then final machining was executed using a milling machine to achieve the final desired dimensions. It is important to note that all the samples were cut parallel to rise which has to do with how the gas bubbles rose in the polymeric material during the process of manufacturing. A random high-contrast speckle is applied on the front surface in accordance with the necessary pattern for DIC and shown in Figure 3.2.

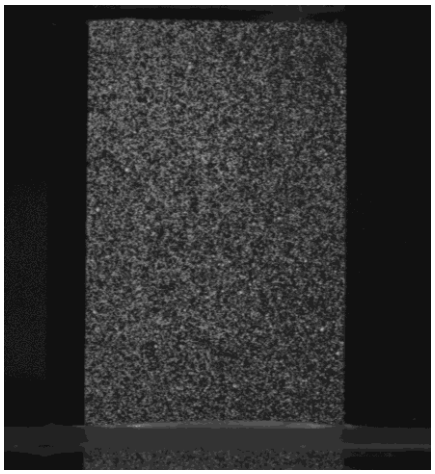

Figure 3.2. Speckle pattern

3.4 EXPERIMENTAL SETUPS

A 5 kN MTS load frame was used for the quasi-static compression experiments. A smaller load cell was needed to obtain more accurate data for the low-density materials but the highest density foam was unable to fully densify using this particular setup. The low rate experiments were conducted under displacement control at an average applied strain rate of 0.001 /s to obtain the loading data. During testing, images were captured at a rate of 1 fps using a 5 MP stereo camera system equipped with 60 mm lenses. The Point-Grey cameras have a full-field resolution of 2448 x 2048 pixel^2. Stereo DIC was implemented in order to account for lateral deformation of the foam. The cameras were at a distance of about 300mm from the specimen and the angle between the two cameras was 12.3º. The complete experimental setup for the quasi-static experiments is shown in Figure 3.3.

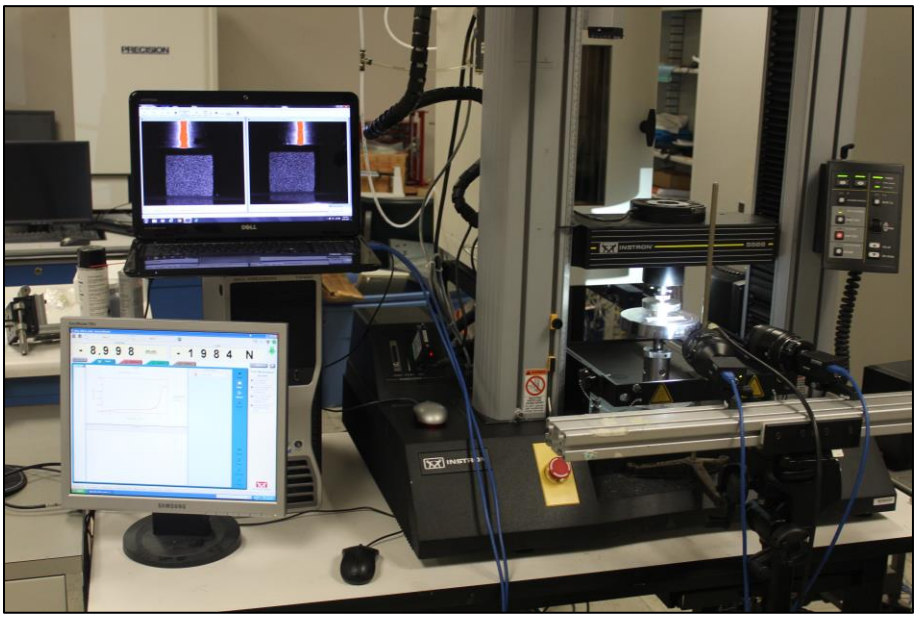

Figure 3.3. Quasi-static experimental setup

The elements of the dynamic testing operation include a dynamic loading device, bar components, data acquisition and recording device, and high-speed imaging system.

The sample was loaded dynamically using a Split Hopkinson Pressure Bar. SHPB is one of the most commonly used experimental setups for strain rates between 10^2 and 10^4 s^{-1}. This dynamic testing method employs stress wave propagation through elastic bars to load a sample and measure the deformation and loading. Standard electrical resistance strain gauges are used to measure the compressive and tensile stress waves propagating through the bars. The schematic drawing and a picture of the experimental setup are shown in Figure 3.4. The SHPB method and its analyses are typically used for testing metals and other high mechanical impedance materials. The uncertainties associated with soft material characterization will be addressed by changing the conventional method. For valid results some modifications had to be made to the standard analyses for testing low mechanical impedance materials, which will be discussed in Section 3.5.2.

Lubrication was used between the sample and bar interfaces to eliminate friction. The low mechanical impedance of the specimen causes the incident bar-specimen interface to act similar to a free surface for the lower density samples. Therefore, most of the incident wave is reflected back and only a small portion of the loading pulse is transmitted through the sample to the transmitter bar. Consequently, the transmitted signal has very small amplitude that can be difficult to differentiate between it and noise. To lessen the impedance mismatch between the specimen and bars, Polycarbonate bars and striker were used amplify the transmitted signal. The use of these viscoelastic bars thereby improves the accuracy of the measurements. The striker bar has a length of 0.45m to achieve large sample deformation. The striker bar is propelled using high pressure helium to generate an elastic stress wave.

To measure the full-field deformation during loading two ultra-high-speed HPV-X2 Shimadzu cameras were used to acquire synchronized images on both sides of the specimen. The cameras were placed at a distance of 0.3 meters from the face of the sample and checked to be planar and parallel to the specimen face. The cameras are capable of acquiring 128 images at the full-field resolution, and for this particular work imaging rate of 200,000 and 625,000 frames per second were utilized, meaning one image was captured every 1.6 and 5 μs. Since 128 images were taken with both cameras the full-field compressive response can only be captured for 204.8 and 640 μs which do not capture the entire deformation since the stress wave is about 730 μs long. The low framerate was used to capture a larger duration of the deformation and the higher framerate was employed to have better temporal resolution, to better capture the displacement during the initial transient time of impact. There is high acceleration during the transient time as the sample goes from being stationary to experiencing high relative motion. This high relative change in particle velocity must be captured for the dynamic evaluation.

The cameras were equipped with a 100-mm macro lens (Tokina) providing an optical resolution of 100 μm/pixel. A high intensity flash monolight (Photogenic) was used to illuminate the area of interest on the sample after trigger from the strain gages. The entire system was triggered using an oscilloscope. The oscilloscope also collected the wave data from the strain gauges through a signal-conditioning amplifier. The projectile velocity was measured using a laser system which found an average of 16.5 m/s.

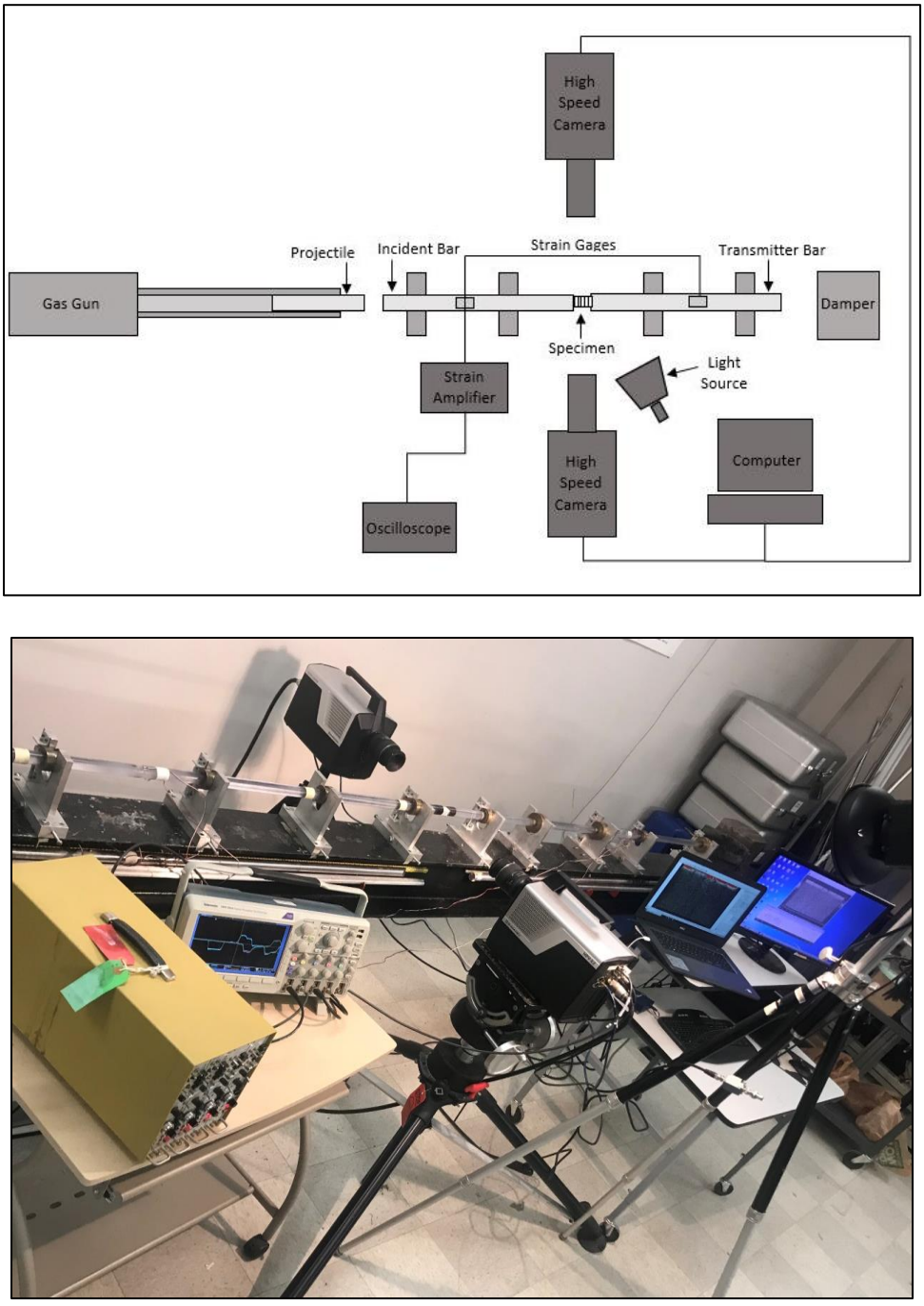

Figure 3.4. Schematic illustration and photograph of dynamic experimental setup

3.5 POST PROCESSING

3.5.1 DIGITAL IMAGE CORRELATION

Digital Image Correlation (DIC) is a non-contact optical technique used to measure the full-field displacement of a surface. A speckle pattern is put on the surface and while being deformed the images taken are used to correlate between the undeformed and deformed state to give the displacement. Then the displacement can be differentiated to find the strain. The images acquired from the quasi-static experiments were processed in the commercial DIC software VIC-3D (Correlated Solutions Inc.). The average speckle size was taken into account to choose the subset and step sizes of 67 and 5. The subset must have sufficient uniqueness and cover at least 6x6 speckles (3 black and 3 white). The center-weighted Gaussian filter was used to derive the strain distribution from the full-field displacement. The correlation criterion was selected to be zero normalized squared difference which is insensitive to the scale of the light intensity, which is necessary since a flash of light is being used. Optimized 8-tap interpolation function was used to convert the discretized point measurements to continuous data.

For the dynamic tests the images were analyzed using VIC-2D (Correlated Solutions Inc.). A subset and step size of 17 and 1 were used for image correlation. The analysis was performed using an incremental algorithm to enable data acquisition for significantly large compressive strains.

3.5.2 FULL FIELD STRESS AND DENSITY CALCULATIONS

The present analysis is based on the assumption of uniaxial deformation. To incorporate the effects of inertia which is known to have a dominating role with soft materials, a new approach is used to define the total axial stress using the full-field

deformation response. Newton's law of motion is manipulated to give the following total stress equation:

$$\sigma_1(x,t) = \frac{F_1(0,t)}{A(0,t)} + \int_{\xi=0}^{\xi=x} \rho(\xi,t) \frac{\partial^2 u_1}{\partial t^2}(\xi,t) d\xi$$

The reconstructed equation shows that the total stress is a location dependent quantity. The first term of the equation is the boundary stress calculated from the transmitted signal. The boundary term is calculated from the transmitted signal using standard one-dimensional wave analysis and time shifted to the bar-specimen interface. The integral term represents the spatial distribution of the inertia stress that is calculated using the displacement data from DIC and material density. The length of the specimen is sliced into 100 segments to acquire the local response. The displacement field is differentiated with respect to space and time to obtain the acceleration field. The acceleration distribution was determined using a finite differences operation and temporally smoothed. The formulation is credible in the event that lateral and shear deformations are negligibly small i.e. the uniaxial deformation assumption is validated.

The foams are highly compressible meaning significant density change is undergone during loading. The density field is calculated as a function of the displacement data obtained from DIC and the initial density, ρ_o. The local density, ρ, at position, *x*, and time, *t*, is found to be:

$$\rho(x,t) = J\rho_o$$

Where *J* is the Jacobian at any point at a given time, which is the transformation from the undeformed to the deformed state. *J* is the determinant of the deformation gradient, *F*, which is determined from the DIC measured displacement field, *d*. More

details on the derivations of these stress and density calculations can be found elsewhere[21].

3.6 RESULTS AND DISCUSSION

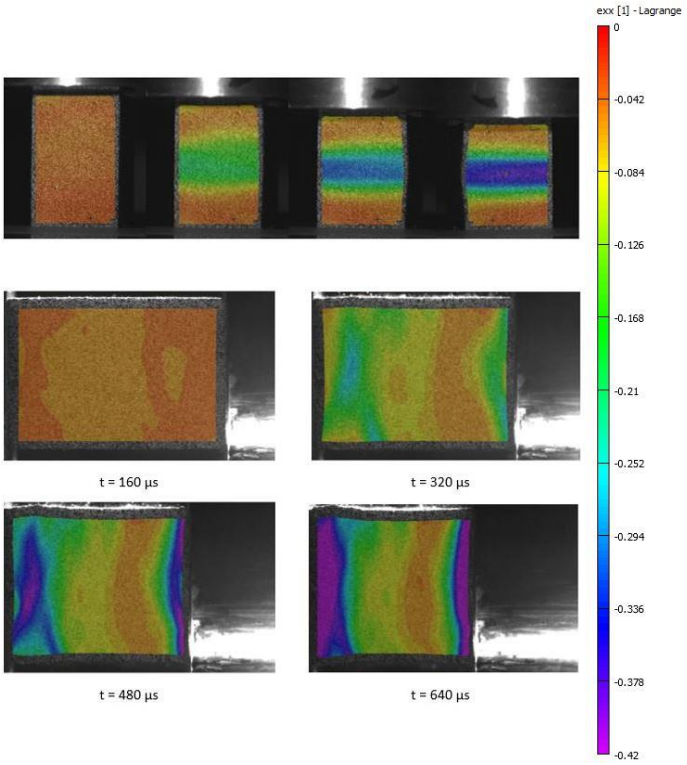

Figure 3.5. Axial strain contour plots of dynamic test of 160 kg/m^3

The evolution of the axial strain on the surface of the specimen is shown in Figure 3.5. It is shown that the deformation is mostly symmetric about the centerline of the sample. Though the non-uniform distribution of strain in the axial direction is clearly noted. The quasi-static stress-strain curves for each nominal density is shown in Figure 3.6. The initial slope of the stress-strain curve is the linear elastic regime from which the Elastic Modulus, *E*, is calculated. This deformation region is controlled by cell wall bending (more specifically, cell face stretching for closed cell foam [22]). The plateau region is associated with the collapsing of the cells. Once all of the cell walls are touching, the cells are completely collapsed and all the void spaces are removed, there is

a rapid increase of stress which is known as the densification stage. This dramatic stiffening of the material happens when the cell wall material itself is being compressed, it acts as a solid.

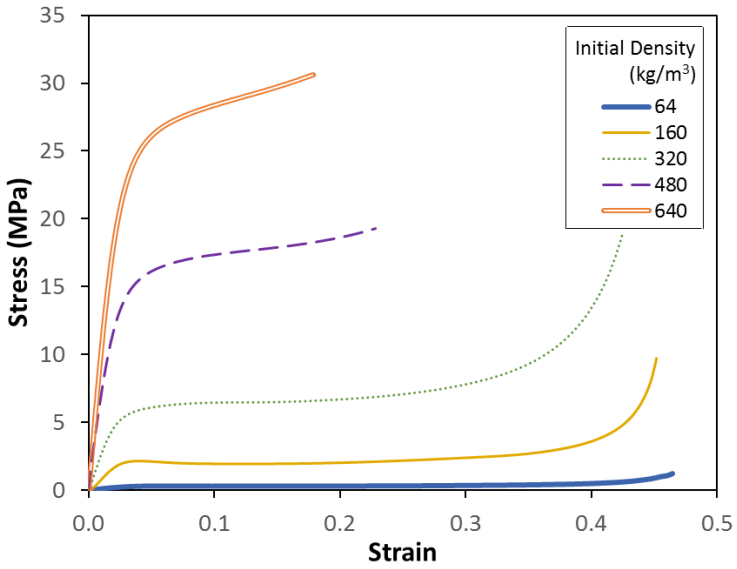

Figure 3.6. Quasi-static compressive stress-strain curve for various densities

It is clear to see that increasing the density of the foam increases the elastic modulus, increases the plateau stress, and reduces the densification strain. Two tests were done for each foam to conclude that the elastic modulus and yield strength values were consistent. The yield point is recognized as the first point on the stress-strain diagram where the strain increases without an increase in strain. It is where the elastic deformation stops and the material begins to deform plastically. The compressive strength is defined to be the stress at the yield point unless it occurs after 10% deformation. If there is no reduction in stress, then the stress at 10% strain is the compressive strength (ASTM standard D1621). The low-density foams exhibit a drop in stress after reaching a peak stress while the higher density foams only show strain hardening. The lowest density

foam has the lowest compressive strength because it has the largest volume of voids, therefore there is a smaller volume of the solid material.

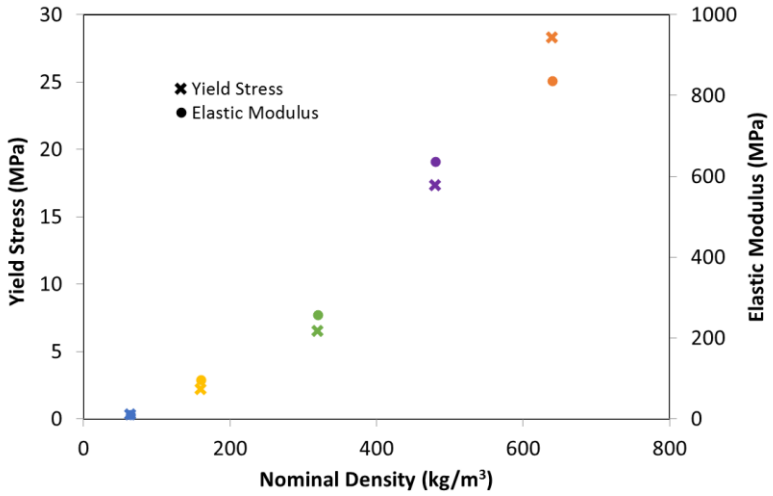

Figure 3.7. Variation of elastic modulus and yield stress as function of density

The distinction between the yield stress and elastic modulus as related to the foam density are depicted in Figure 3.7. A linear relationship is observed for these mechanical properties. It is important to remind the reader, that even though the highest density sees higher yield strength, that does not make it the ideal foam. The end goal is to have the most efficient energy absorbing structure, which means a large area under the stress-strain curve is what is truly desired.

Next the results of the dynamic experiments are investigated. Figure 3.8 shows the incident and transmitted signals from the strain gauges for the lowest and highest density foams. The lowest density has very little transmitted stress, the material is so soft that the interface acts similar to a free surface, almost all of the wave is reflected. Note that the transmitted signal in Figure 3.8.a is magnified x5. Whereas the highest density foam has a very small reflected wave and a very large transmitted wave. Using one wave analysis the boundary stress was calculated from the transmitted signal.

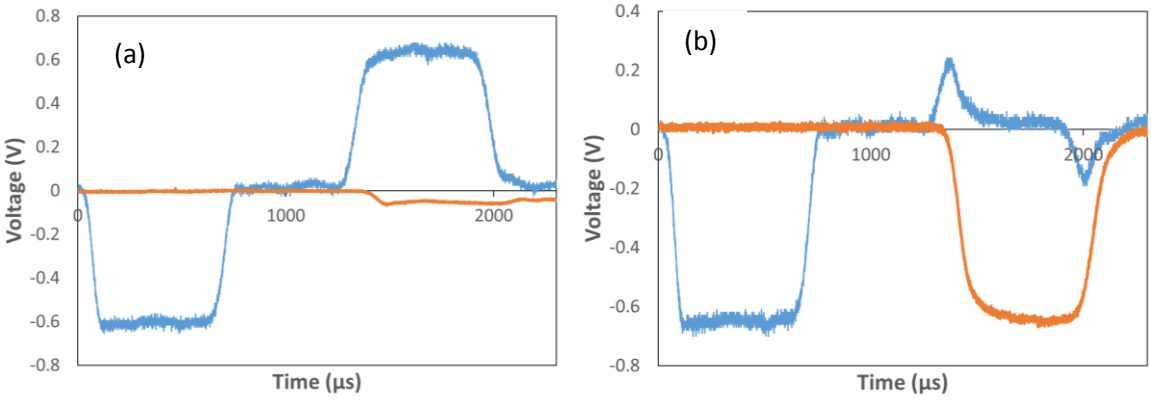

Figure 3.8. Oscilloscope voltage signals of dynamic compression tests for (a) 64 and (b) 640 kg/m^3 foam densities

The axial acceleration along the specimen axis was calculated by taking a double derivative of the axial displacement that was recovered from the camera taking images every 1.6 µs. This high framerate has better accuracy to not filter out any data during the transient loading process. The spatial variation of the axial acceleration for different times is shown in Figure 3.9. The acceleration curves increase everywhere along the length of the specimen up to 30 µs, and then the acceleration starts to come down. In Figure 3.9.b the acceleration curves are observed to oscillate around the zero axis. This shows that the foam is performing its desired function of damping the peak accelerations.

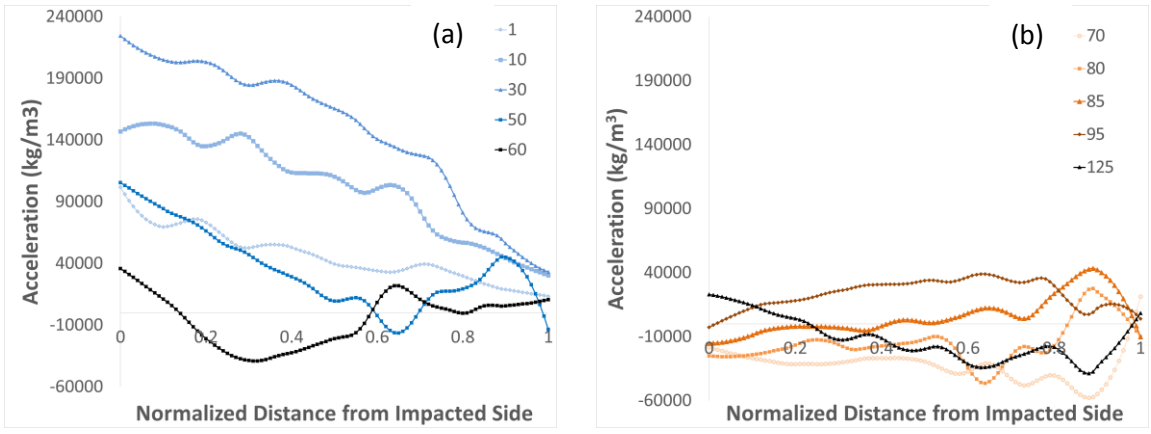

Figure 3.9. Acceleration curves of 160 kg/m^3 foam for the (a) first half of the test and (b) the second half

The axial acceleration for all five foams is shown in Figure 3.10. All five of the foams follow a similar trend but the magnitudes slightly vary. Since all of the materials experience the same force for the same time duration, but have differing masses it would be expected that the displacement would vary causing the acceleration to be different. It is shown that the peak acceleration diminishes as time goes on. Those oscillations seen after the peak acceleration are in all probability just noise from the displacement data. When the acceleration becomes negative signifies that the stress wave has reached the end of the length of the specimen and reflects back. It is observed from these acceleration curves that during the transient deformation stage there occurs a rapid increase in particle motion.

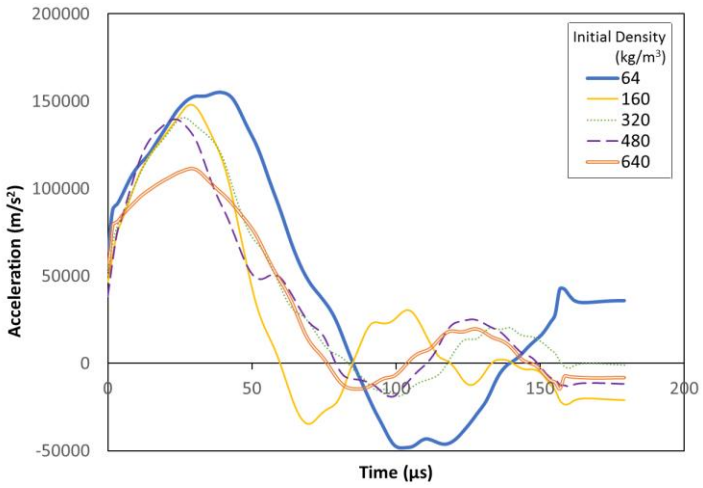

Figure 3.10. Acceleration for all five foams

The spatial distribution of the axial inertial stress is calculated using the previously given equation with the functions of acceleration and local density. The spatial variation of the inertia stress along the length of specimen is depicted in Figure 3.11 for different times. Similar to what was observed with the acceleration curves in Figure 3.9, the maximum peak occurs within the first 30 µs at the impacted end.

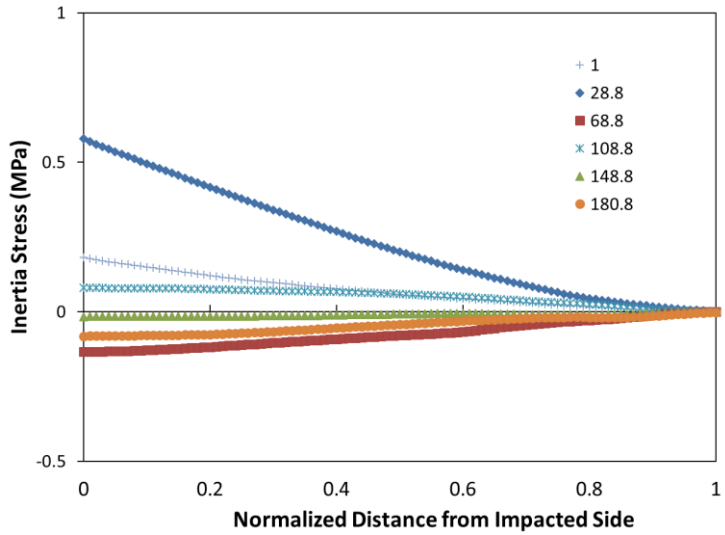

Figure 3.11. Inertia stress for 160 kg/m^3

The positive inertia stress is compressive for this work, which when added to the boundary stress will increase the overall axial stress. The observed inertia stress is clearly significant at the impacted end and cannot be ignored for these foam materials. The inertia stress is added to the boundary stress measured from the transmitter bar using the previously given equation. The added inertia term results in the appearance of a spike in the stress in the initial portion of the stress curve.

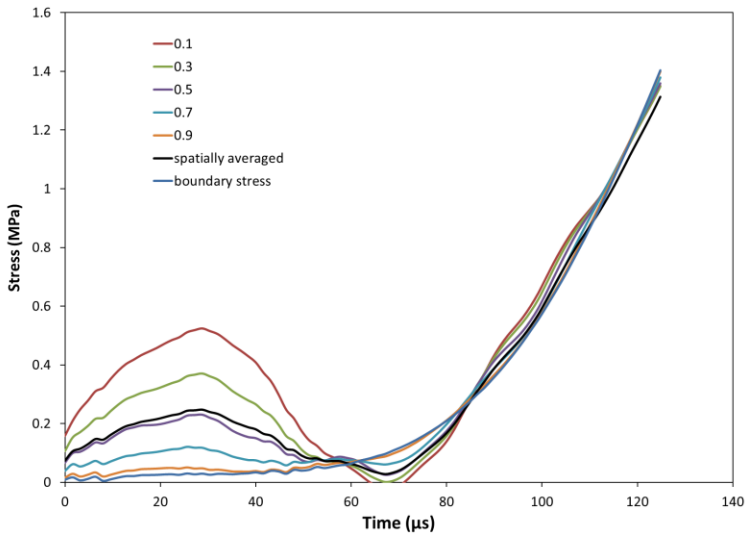

Figure 3.12. Superimposed inertia and boundary stress for each layer for 160 kg/m^3

Figure 3.12 shows the local evolution of the total axial stress at five different points along the specimen length. Substantial variation is observed during the first 80 µs after impact. The spatial variation decreases at longer durations due to the acceleration damping out. Even though the stress and strain vary locally along the specimen length, it is the global stress-strain curve that is needed to determine the specific energy. The local stress curves are spatially averaged and are shown in the graph to give the effective average constitutive response. The total stress-strain curves for all the foams are given in Figure 3.13. The global strain was directly output using DIC. Also, it should be noted that the stress referred to throughout this work is the engineering stress since the true stress cannot be calculated because it assumes that the volume remains constant which is not valid with these compressible materials.

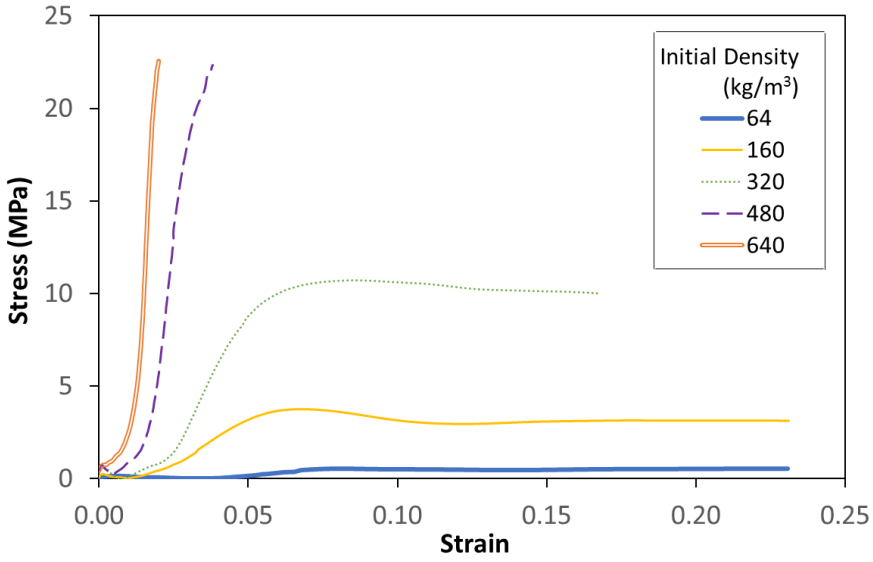

Figure 3.13. Stress-strain curve for dynamic tests

The depicted stress-strain curve is only for the first 640 µs, since that is the duration of the images being captured to find the global strain. The inertia stress intensifies the SHPB measured stress during the early transient time. The plateau stress

plays the biggest role in energy absorption. The highest density reaches the highest maximum stress but densification begins at a very low strain. The lowest density has a very long plateau stress, it experiences very large deformation but at the compromise of a very low maximum force. The strain energy density (the strain energy per unit volume) is calculated by measuring the area under the stress-strain curves. This value is graphed as a function of stress and strain in Figure 3.14.

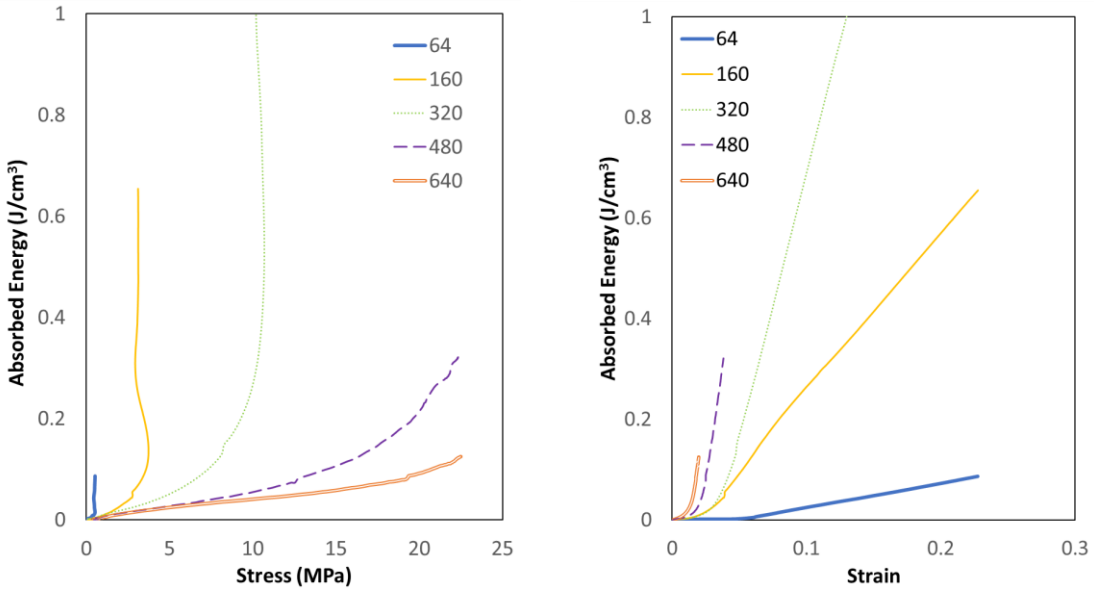

Figure 3.14 Energy absorbed as a function of stress and strain

For a predefined stress design criterion, as the desired stress is increased, the increasing density foam becomes the next ideal foam. For 1 MPa stress, the lowest density foam as the highest amount of energy absorbed, but for a stress of 23.5 MPa, the highest density would be the selected foam. The opposite matter is true for a specific level of strain. For smaller strain, the 640 kg/m^2 is "better, but for a large amount of deformation the 64 kg/m^2 would be chosen. The increase in plateau stress is shown for the dynamic as compared to the quasi-static tests in Figure 3.15. This apparent strain rate sensitivity is reliant upon the viscoelastic nature of these polymeric foams.

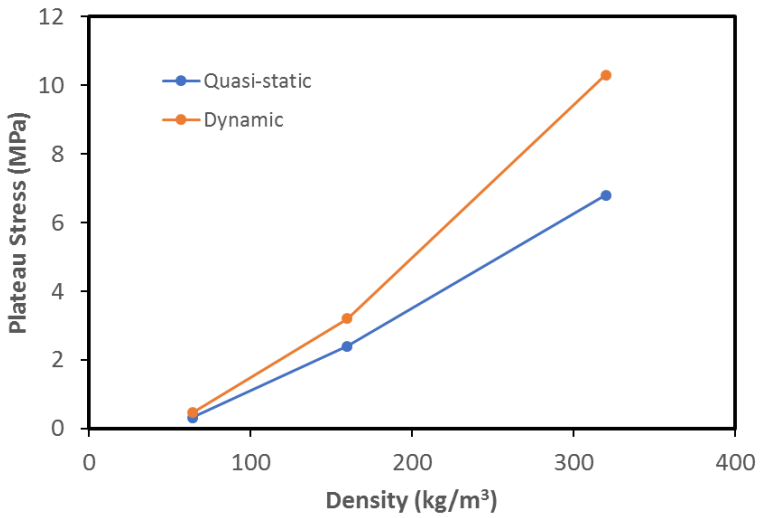

Figure 3.15. Strain rate sensitivity of three lowest density foams

3.7 CONCLUSIONS

The energy absorption of five different density foams is found experimentally for low and high strain rates. A servo-mechanical load frame and Split Hopkinson Pressure bar are used in conjunction with Digital Image Correlation. For accurate results with SHPB the best approach is to have uniform deformation at an equilibrated stress state and constant strain rate. None of these conditions are present for a soft material under dynamic loading. A new method that takes account of the inertia effects and compressibility of the sample is applied in this work. The stress-strain response of each material is calculated to determine the mechanical properties and constitutive response of the homogeneous foams. The stress-strain response clearly has a strong relation to the density of the foam. The elastic modulus and yield strength increase with increasing density, and the densification strain decreases. This stress-strain relationship is also indicative of the correlation between the density and the energy absorption. The material is also shown to have high strain rate sensitivity, the response gets stiffer with increasing strain rate.

CHAPTER 4

DENSITY GRADED FOAM COMPARISON STUDY

4.1 ABSTRACT

The improvement of energy absorption with graded cellular materials is investigated through experimental techniques. Dynamic testing of polymeric foam is performed using Split Hopkinson Pressure Bar (SHPB) and Digital Image Correlation. The validity of dynamic loading conditions depending on homogenous stress distribution is overcome by including the effects of inertia. The dynamic stress equilibrium equation is utilized with a boundary stress measured from the SHPB while the deformation of the entire foam specimen is recorded with high speed photography. The data is mathematically processed in order to draw the characteristic stress-strain curve. Results indicate that the layered structures yield an improved energy absorption compared with monolithic foam under specific design criterion.

4.2 INTRODUCTION

Functionally graded materials are in the family of engineering composites that are designed for a specific function. There has been a considerable amount of numerical work done to characterize the dynamic deformation of FGMs but a lack of experimental study is noticed. This has to do with the many challenges with high strain rate testing of soft materials that make it difficult to achieve an acceptable characterization of this response. So there are already many issues that come into play with dynamic testing of foams, let alone a soft material with density gradation. The non-equilibrated stress is a

result of the axial inertia, which will be taken into account in the analysis of this work. The concept of Functionally Graded Foam Material (FGFM) has been introduced to improve upon certain properties as compared to a homogenous foam. The appeal of FGFM is to enhance the energy absorption characteristics due to the presence of the high-density foam, while maintaining a low structural weight. A graded structure with 5 different densities is examined.

4.3 MATERIAL AND SPECIMEN GEOMETRY

The five distinct layers of different bulk densities form the samples prepared in house, which are made from the uniform foams used in Chapter 3. Each layer of polyurethane foam was machined to 17×17×5 mm^3 and then polished using silicon carbide papers to have a smooth surface, suitable for speckling. The layers were bonded together with a thin layer of highly-flexible polyurethane adhesive. It is vital that the adhesive is flexible to account for small relative lateral deformation of the layers and to minimize shear stress developed within the interface. The final length of the specimens is 25 mm. A schematic of the arrangement of the layers along with a picture are shown in Figure 4.1.

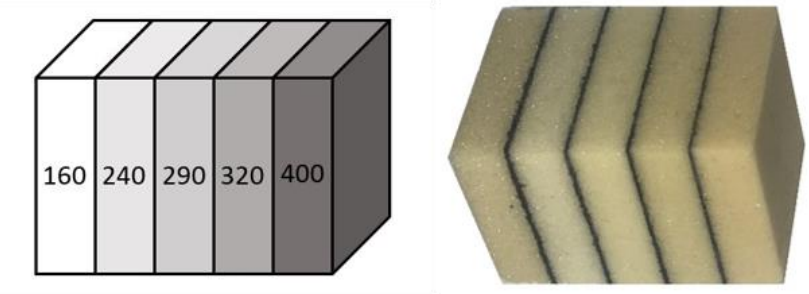

Figure 4.1. Graded foam schematic and photograph

Before speckling, a marker was used to draw a line between the layers to indicate the interfaces. A small piece of tape was used to cover part of the front surface before

speckling to leave a strip unpainted to help distinguish the different layers during deformation. The front surface of the specimens was painted white and then black speckling was applied using conventional spray painting method. The same experimental methods were used for quasi-static and dynamic testing of the five-layered density graded structure.

4.4 RESULTS AND DISCUSSION

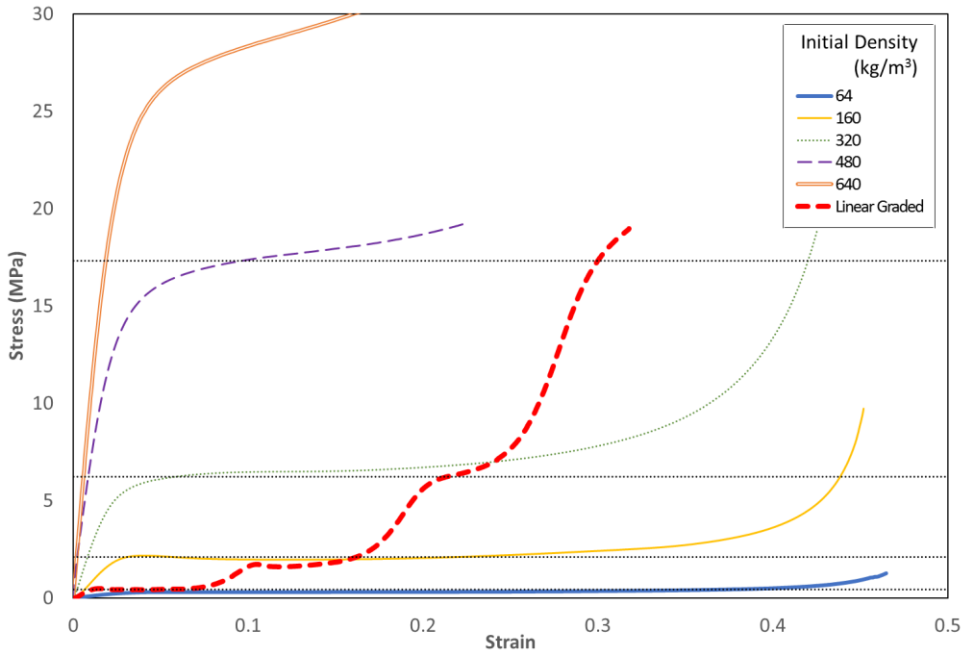

Figure 4.2. Stress-strain curve for quasi-static tests

The quasi-static stress-strain response for the graded structure is shown in relation to the uniform foams in Figure 4.2. Each of the incremental stepwise plateaus correspond to the plateau stress of that corresponding uniform foam. Figure 4.3 investigates the energy absorption compared with the five uniform foams.

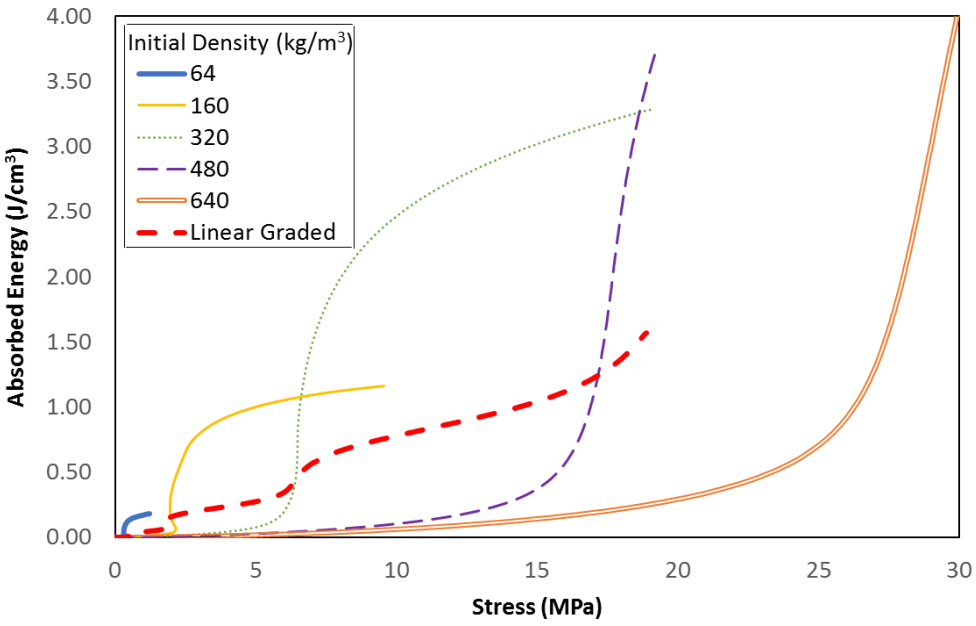

Figure 4.3. Absorbed energy as function of stress for quasi-static experiments

The graded foam shows improved energy absorbance performance compared to each homogenous foam up until the uniform foam curve intersects the graded foam curve and the absorbed energy increases dramatically. This initial improvement could be due to the extended plateaus provided by the low-density layer. It is noted that each time the absorbed energy curve sees a rise it intersects the corresponding uniform foam curve.

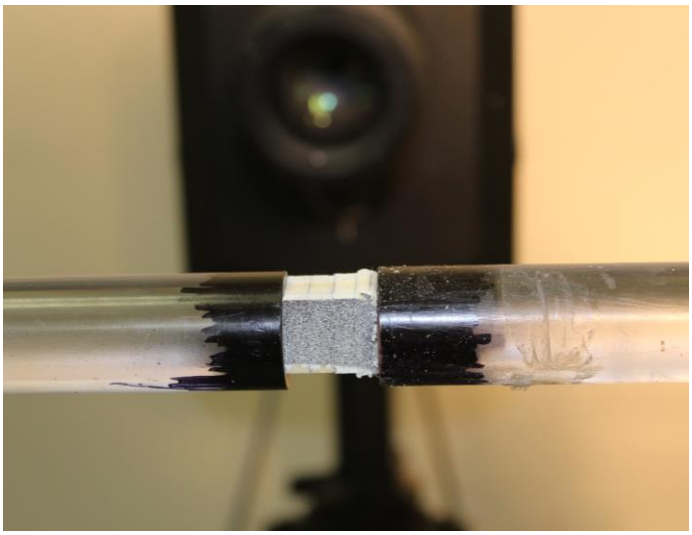

Figure 4.4. Picture of deformed specimen

Next the dynamic response of the graded foam as compared to the uniform foams is presented. A photograph of the specimen after deformation is shown in Figure 4.4 to examine how the layers deformed. It is noted that the entire sample was not completely deformed, only the first three layers completely failed. This was not a characteristic of the structure but rather not a large enough load was applied to crush the highest density layers.

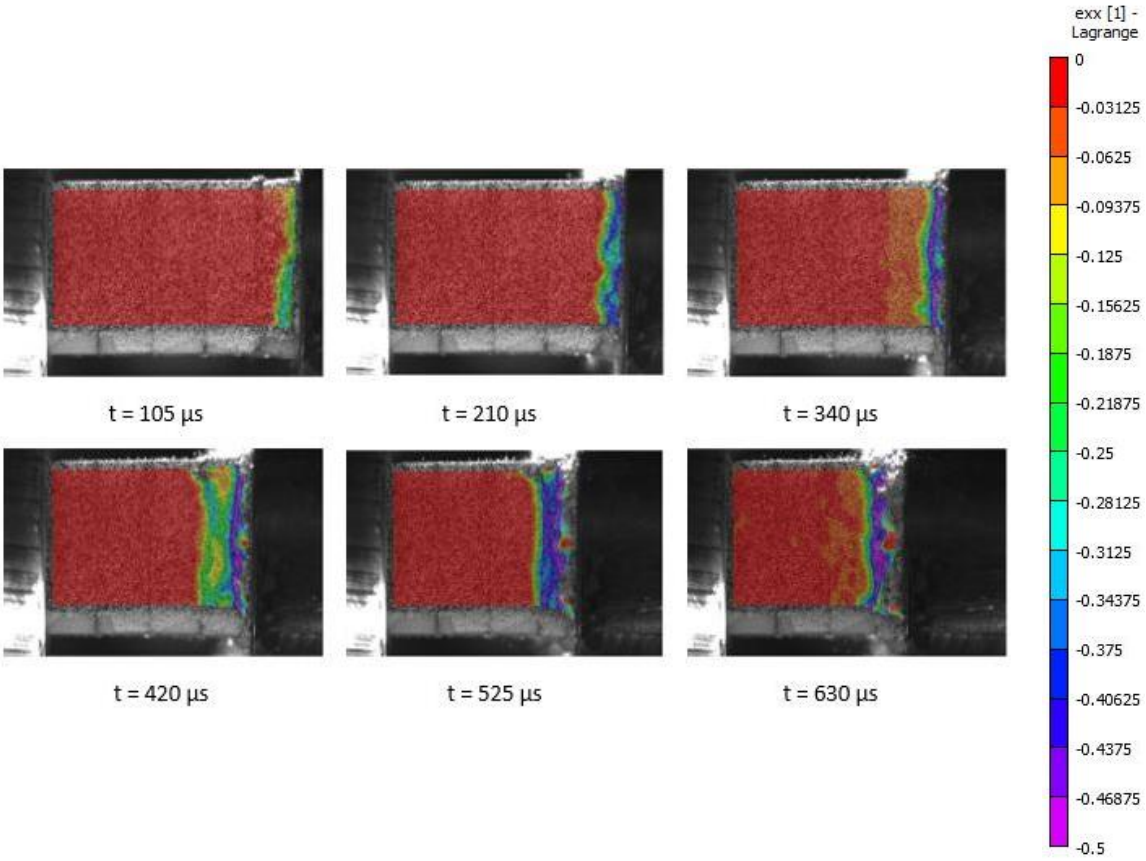

Figure 4.5. Axial strain contour plots

The contour plots show the axial strain distribution in Figure 4.5. The difference between the strains in each layer is easily seen. The lowest density layer completely crushes before the distal end of the specimen has even been exposed to the stress wave. The local strain from each layer is plotted in Figure 4.6. It is evident that the strain is not

homogeneous along the length of the specimen. Each layer is strained in a stepwise order starting with the lowest density. While the first layer is being crushed, the rest of the layers see very little strain, and once it has failed, the next layer begins to strain, a dramatic increase in the strain can be observed. There is very little change in the strain for the two highest density layers.

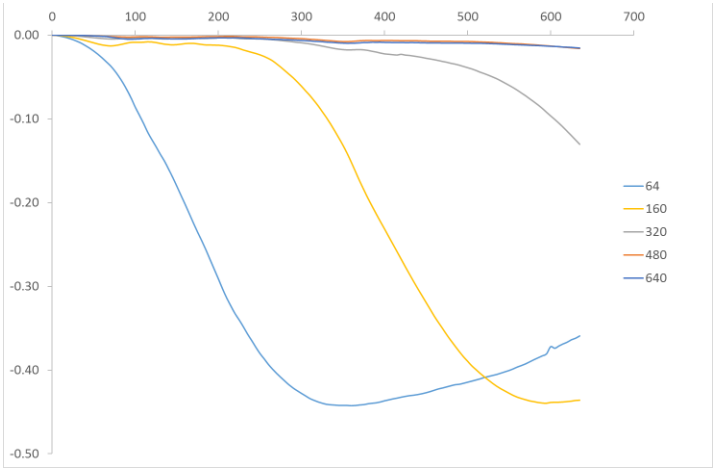

Figure 4.6. Local Strain plot

The stress measured from the transmitter bar using the SHPB technique is displayed in Figure 4.7. The uniform foams from the previous chapter exhibited a near constant plateau stress while the graded foam shows a smoothly rising plateau stress. The stress wave propagating through the layers can be seen as the increasing steps. Also, it is remarked that for the first 80 μs the stress is near zero because the transmitter bar is not exposed to the stress wave yet, though deformation has already begun to occur at the impacted end. The signal to the strain gauge is delayed due to the super-low impedance of the soft layer.

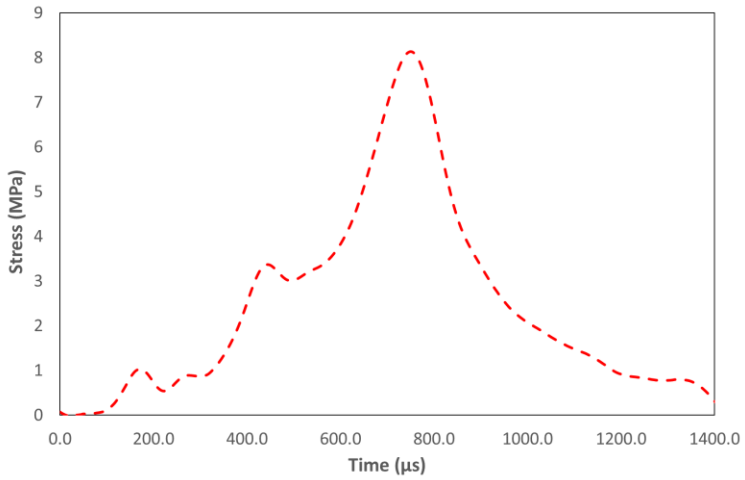

Figure 4.7. Boundary stress measured from strain gauges

The inertia stress is calculated for this transient duration while accounting for the layers of different initial densities. It was added to the boundary stress to give the following total stress-strain curve in Figure 4.8. The graded foam was compared with the two low density foams since those were the two layers impacted and failed. The inertia stress was found to have a slightly higher magnitude as compared to the 64 kg/m^3 density foam, which was the first layer impacted for the graded foam.

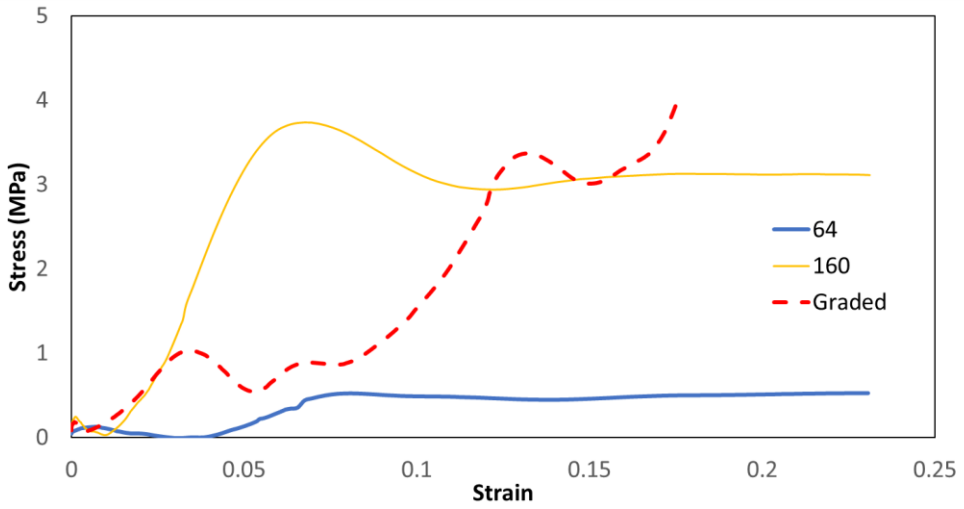

Figure 4.8 Total dynamic stress-strain response compared to uniform

Similar to the quasi-static stress-strain curves, a stepwise increase in the flow stress occurs at certain stress levels. Due to the framerate of the cameras, the entire global strain during deformation could not be captured, so only the lowest density uniform foams are shown in Figure 4.8 for comparison with the graded foam. The peaks in the graded curve seem to correlate with the compressive strength of the uniform foams.

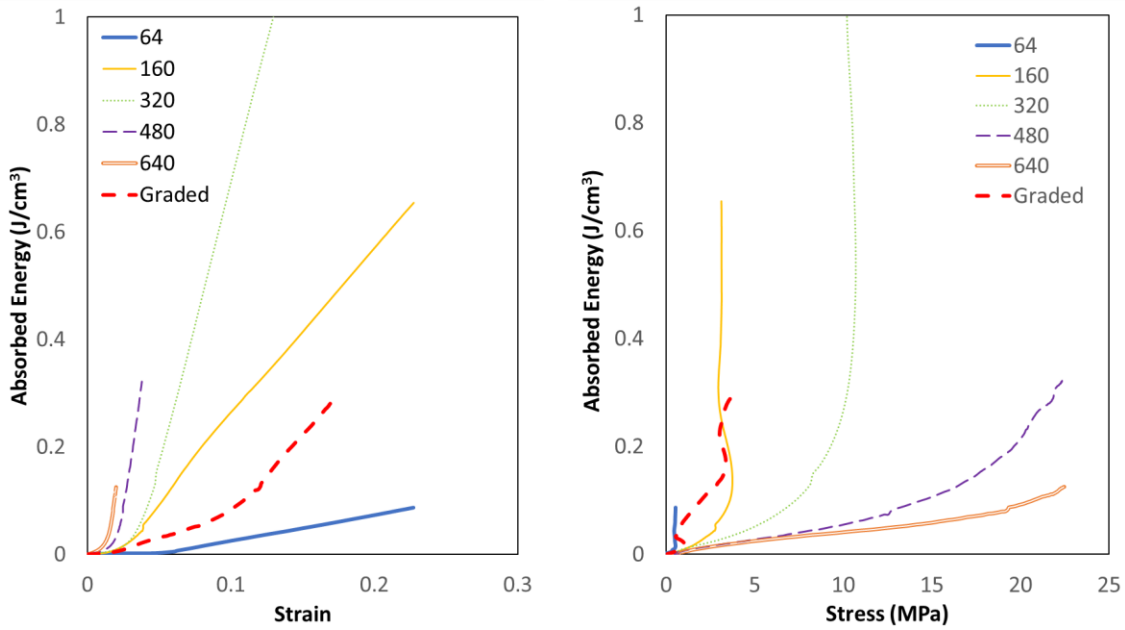

Figure 4.9 Energy absorbed as a function of stress and strain-graded compared to uniform

The absorbed energy in relation to the stress and strain is investigated in Figure 4.9. It is observed that for certain stresses and strains, the graded foam does show improved energy absorption over each homogenous foam. For a very small stress, less than 0.5 MPa, the lowest density shows the highest amount of energy absorbed, but then up to 3 MPa the graded foam exceeds the rest of the foams. For a predefined strain the graded foam appears to only show improvement over the lowest density. Though if the desired amount of deformation is greater than 4% the graded foam would be ideal over

the two highest densities because they see very little strain before the material fully densifies.

4.5 CONCLUSION

The constitutive response of a functionally graded foam material compared to homogeneous cellular materials was studied. Quasi-static and dynamic tests were conducted to investigate the stress-strain response. The temporal evolution of the sequential localized deformation of the material along the axial direction was observed using DIC. Synchronization of the oscilloscope signals with the digital image recordings enables measurement of the total dynamic stress-strain response. This method has made it possible to evaluate the non-equilibrium state of stress for these low impedance materials. The density distribution was seen to have a significant effect on the mechanical response. Depending on the design criterion the graded foam shows improved energy absorption over uniform foams for certain cases Specifically if the application of the structure requires a small stress, the linear graded foam shows superior energy absorption over the uniform foams.

CHAPTER 5

EFFECTS OF STACKING SEQUENCE ON ENERGY ABSORPTION OF GRADED FOAMS

5.1 ABSTRACT

Different bulk density polymeric foam layers are bonded together in different stacking arrangements and subjected to impact loading. Ultra-high-speed imaging is implemented to measure the deformation and observe the formation and propagation of the stress waves during direct impact. The arranging of the layers' effect on energy absorption is explored. The optimum FGM configuration will depend considerably on the critical design conditions for the specific application.

5.2 INTRODUCTION

Polymeric foams are cellular materials that in many industries such as aerospace, automotive, and military have become of great deal of interest. These cellular structures are ultra-light solids which absorb substantial energy in compression. Their many applications involve absorbing impact and shock mitigation through energy dissipation by progressive local crushing. It is well known that energy absorption is strongly related to the foam density. Functionally Graded Materials (FGM) are advanced engineering materials that enable a material to have the best properties of multiples materials. The significant advantage of functionally graded foam materials is the optimization of strength to weight ratio. It is well established that higher density results in higher

strength. Graded foam has the appeal of higher strength (higher density) combined with lighter weight (lower densities).

The advent of graded foam has mostly been analyzed through simulations and analytical works. The numerical representations of graded foam have for the majority been analyzed through gradient functions. Cui [2] tested the variation of gradation of the foam characteristics with finite element simulations and found improved performance over single-phase foams. Kiernan [5] developed a finite element model of the SHPB to study the wave propagation through FGFM's. The impact response of density graded cellular polymers has been analyzed by observing the propagation of compaction waves using DIC [23]. Zeng [24] studied the influence of the density gradient on the energy absorption capacity of graded polymeric hollow sphere agglomerates. The ideal gradient architecture for optimal design of graded polymeric foams in energy absorbing applications is investigated in the present work. It is shown that the placement of these layers in reference to the side being impacted vs. the side in contact with the object being protected makes a difference in the mechanical response under dynamic loading.

5.3 MATERIALS AND SPECIMEN GEOMETRY

Discretely layered specimens were made with 5 different bulk density foams. The different sequences studied took on either a linear stepwise or sandwich configuration as the following stacking arrangements: 64/160/320/480/640, 640/480/320/160/64, 64/480/640/480/64, and 480/320/64/320/480 kg/m^3. The layups were chosen to all have similar weights for comparison. A picture of the two sandwich configurations is shown in Figure 5.1. The linear increasing density was shown in Figure 4.1 and the linear

decreasing gradation is the same sample just flipped in the test frame. The same experimental method for dynamic testing was used as in the previous chapters.

Figure 5.1 Pictures of sandwich orientations

5.4 RESULTS AND DISCUSSION

The contour plots of the axial strain spatial distribution are shown for each orientation at the same global strain in Figure 5.2. It is clearly observed that as would be expected, in every instance, the lowest density foam is the first to fail. After complete densification of the lowest density layer deformation moves on the next highest density layer. The middle-high arrangement had the lowest density layer on both ends and it is worth noting that the impacted end was showing a higher strain value.

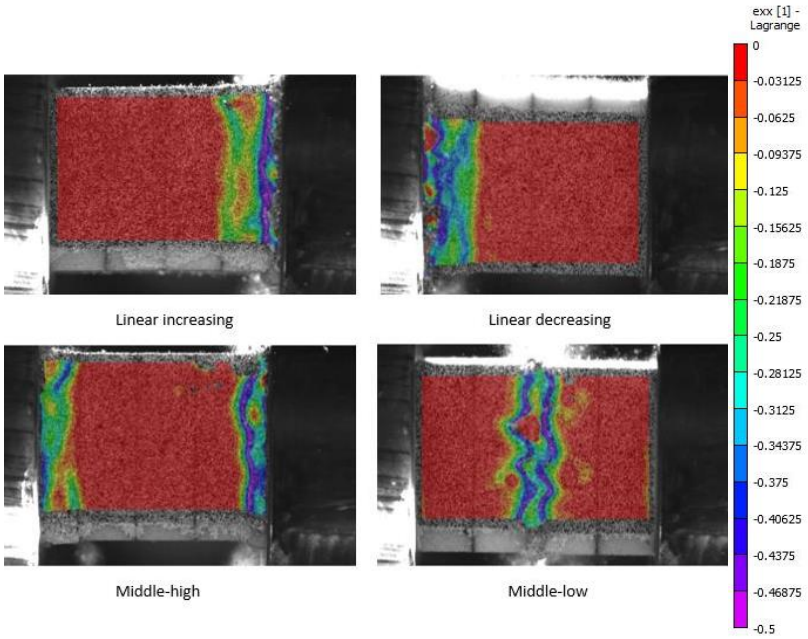

Fig 5.2. Axial strain contour plots

The local strain evolutions obtained from each layer for the two linear gradations are presented in Figure 5.3. The heterogeneity of the strain distribution is clearly observed. There appears to be a small but important time delay for initiation of strain in the lowest density layer when it is farthest from the impacted end. This time delay could improve the failure response of the structure because it could lead to a time delay for damage to initiate. Kiernan [5] observed this same time delay, deducing that a decrease in density (decreasing the yield stress) will allow for greater amount of energy to be absorbed plastically. Also, it is observed in the figure that the second highest density layer is slightly strained before the lowest density layer is fully densified when it is exposed to the stress wave first (decreasing density arrangement). Alternatively, with the linear increasing density, each layer begins to strain once the previous lowest density layer is fully densified.

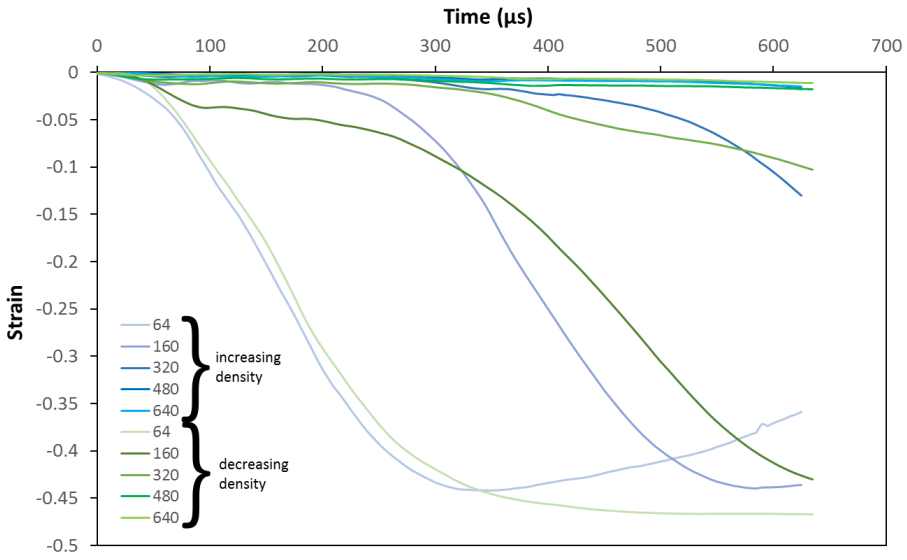

Figure 5.3 Local strain plots for linear gradation

The inertia stress is superimposed with the boundary measured stress to give the total global stress. This stress is plotted with the global axial strain extracted from DIC in

Figure 5.4. Again, it should be noted that the full structure wasn't completely failed and the equilibrium state was not reached. From the figure it can be seen that at the very early stage of the tests there is a large variation of the stress due to the inertia effects. The large plateau of the middle-high sandwich configuration is nearly identical to that of the 64 kg/m^3 foam which makes sense because the configuration has two layers of that low-density foam. The initial part of the middle-low curve is very similar as well but at 13% strain there is a dramatic increase in the stress because the 64 kg/m^3 layer has fully failed and the next highest density is a much larger step increase of the density as compared to the other orientations. It reaches the smallest total strain because the final strain depends on the crushing level of the nest weakest layer. The two sandwich configurations are nearly opposite in their stress-strain response. The middle-high layup sees large strain but small stress, while the middle-low sees small strain and large stress.

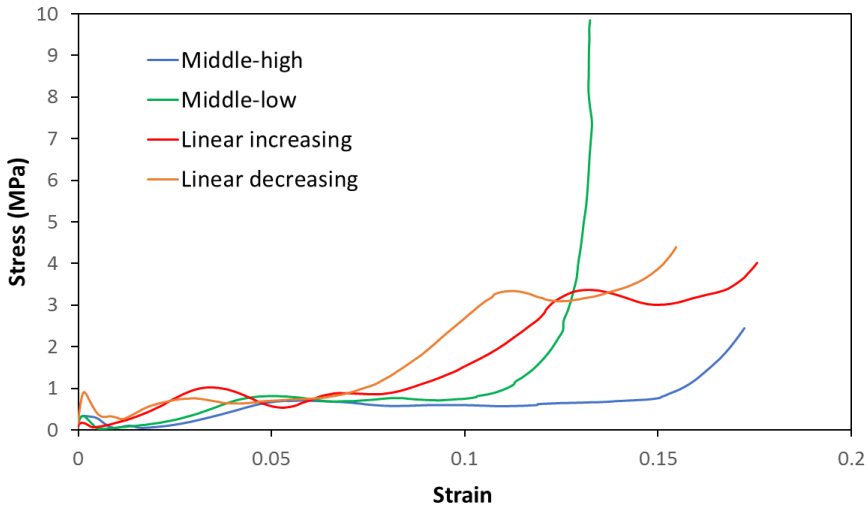

Figure 5.4. Total Stress-Strain

The area under the curve is calculated to find the energy absorbed. Since the total loading and unloading of the specimen is not captured, two different possibilities are offered to compare the four options. If the design criteria are based upon a predefined

stress or strain, the following graphs portray the comparison of energy absorbed for the four different configurations. The absorbed energy as a function of stress is depicted in Figure 5.5 and as a function of strain in Figure 5.6. These plots are used in order to obtain a relative comparison of these stacking arrangements for a fixed time duration.

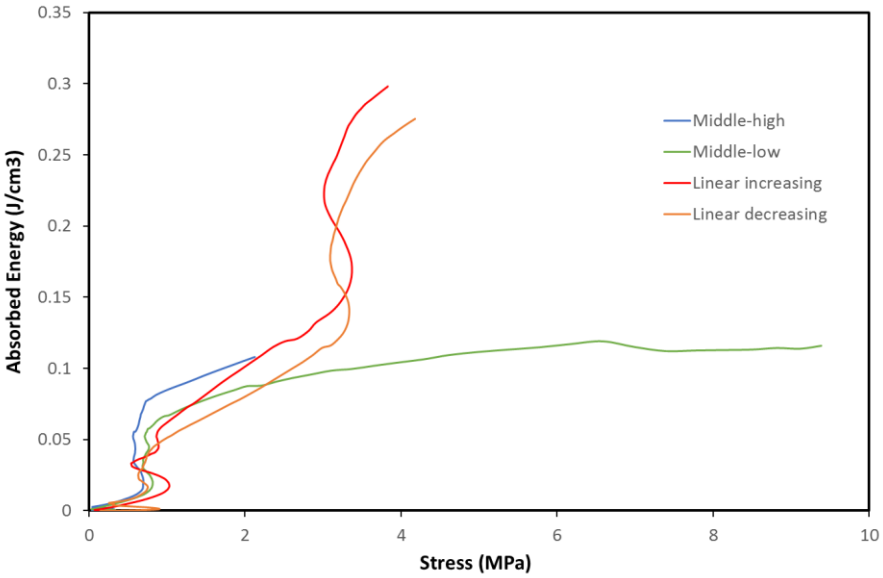

Figure 5.5 Energy absorbed for predefined stress

The middle-high orientation shows higher energy absorption for a small stress, up to about 2 MPa, which can be attributed to the double layer of the lowest density foam. The lowest density layers would support extended plateaus which subsequently promotes higher energy absorption. With an increase in transmitted stress, the middle-low layup sees very little increase in amount of energy absorbed. Overall the two linear gradations see the highest amount of energy absorbed for this duration of impact. If there is a specific amount of deformation that is desired, the following plot shows the comparison of energy absorbed for a defined strain.

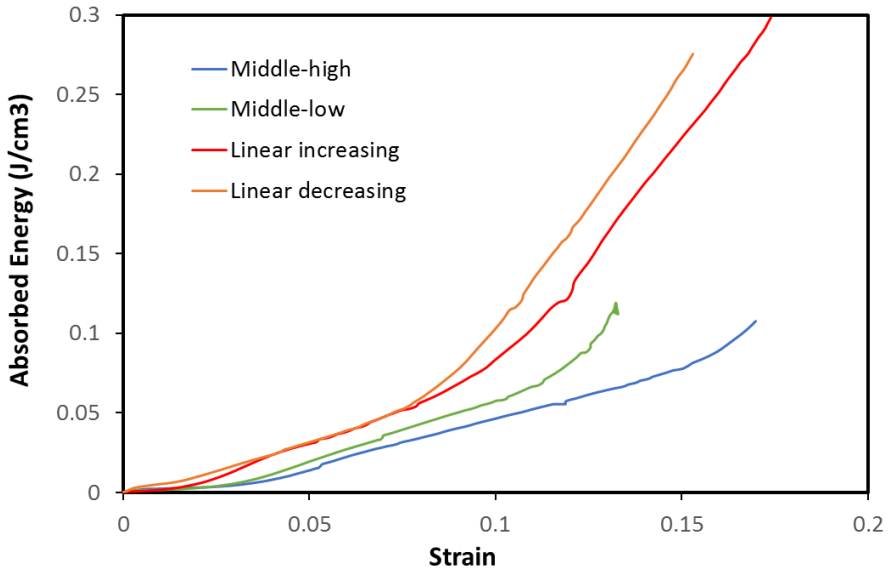

Figure 5.6. Energy absorbed for predefined strain

Obviously the linearly decreasing configuration is the desirable layup for this design criterion up to a strain of 15%. This greater energy absorption could be an effect of the time delay that was observed in Figure 5.2. It is intuitive that the middle-high would see the smallest amount of absorbed energy for a specific strain because the structure sees a very small stress due to the presence of the 64 kg/m^3 layers. Owing to the small stress, even at larger strains, befalls a small specific energy magnitude. If the design criterion would be to attain a certain amount of deformation, for strains less than 17% it is apparent that the sandwich structures would not be the ideal candidates.

5.5 CONCLUSION

The ability to tailor the morphology of these cellular materials to improve energy absorption will increase the safety standards in the many applications that these materials can be used. Ultimately, the final goal is to have a predictive model for graded foam that can be used in design tasks intended for impact loading environments. It is shown that the gradient does in fact play a role in the energy absorption for these heterogeneous

materials. Regardless of the arrangement of the layers, the lowest density layer is always the first to fail. So, one advantage is that by rearrangement of the layers comes the ability to force the initial crushing to occur at a predetermined region. In order to compare four different stacking arrangements, there is a fixed time duration for the resulting data. The strategy to have the most energy absorbed for a small predefined strain would be to have the highest density, the hardest material, at the impacted side and a linearly decreasing gradation to the structure that is being protected. For the case of a stress less than 2 MPa, the middle-high layup would be the most suitable. For these two cases, the desirable trait is to have the softest materials in contact with the material being protected. Intuitively that sounds ideal to have the softest material cushioning to protected object to reduce injury. But taken as a whole, the linear graded arrangement saw the highest magnitude of absorbed energy, regardless of which way it was oriented.

CHAPTER 6

SUMMARY AND RECOMMENDATIONS

6.1. SUMMARY

Functionally graded materials have the advantage of achieving tailored morphologies for desirable structural properties. The goal is to optimize the stacking arrangement of layers of different bulk densities for superior energy absorption. Rigid polyurethane foams were investigated at low and high strain rates. First the uniform foams were individually tested to get each material's constitutive response. High strain rate experiments were conducted on specimens that were fabricated in the lab and deformed using a standard SHPB. The compressive deformation behavior was observed using high-speed cameras and image correlation software. The full-field displacement was implemented to calculate the inertia effects and material compressibility. The inertia stress was shown to be significant during dynamic loading, confirming the idea that the SHPB analysis would be inaccurate since it uses the assumption of zero inertia effects. Also, it was verified that there is substantial spatial variability in stress and strain for these low impedance specimens. The full-field strain maps extracted from DIC were used to evaluate the mechanical response of the graded sample. By rearranging the configuration of the density gradation compared to the loading direction, a variation in the densification and strain progression occurs. These deformation characteristics will be used to tailor the material to a specific load and timeframe.

The relative density is observed to have a distinct influence on the energy absorption. The proposition of graded foams having the advantageous characteristics of different densities was a productive effort. It is found that graded foam materials do have enhanced characteristics over homogenous foams for certain cases. The wanted energy absorption improvement was confirmed for specific loading and deformation conditions using experimental methods.

6.2. RECCOMENDATIONS

It is recommended that this study continue to be explored. The optimization of enhanced energy absorbing foams could serve to improve many engineering applications of cushioning structures. It would also be advisable to use stereovision DIC for the dynamic tests to look into any radial inertia effects. The tests should be extended to include more stacking arrangements and variations of the thickness of each of the layers, as well as all of these orientations should be tested at varying strain rates. It would be interesting to see the effects of strain rate, if at a certain strain rate one configuration becomes better than another. With the advances in fabrication methods, the experiments could eventually include the study of continuous foams.

REFERENCES

[1] Zhu F, Chou CC, Yang KH. Shock enhancement effect of lightweight composite structures and materials. Compos Part B Eng 2011;42:1202–11. doi:10.1016/j.compositesb.2011.02.014.

[2] Cui L, Kiernan S, Gilchrist MD. Designing the energy absorption capacity of functionally graded foam materials. Mater Sci Eng A 2009;507:215–25. doi:10.1016/j.msea.2008.12.011.

[3] Wismans J, van Dommelen J. Characterization of polymeric foams 2009.

[4] Avalle M, Belingardi G, Montanini R. Characterization of polymeric structural foams under compressive impact loading by means of energy-absorption diagram. Int J Impact Eng 2001;25:455–72.

[5] Kiernan S, Cui L, Gilchrist MD. A numerical investigation of the dynamic behaviour of functionally graded foams. IUTAM Bookseries 2010;19:1–9. doi:10.1007/978-90-481-3771-8-2.

[6] Zhang X, Zhang H. Optimal design of functionally graded foam material under impact loading. Int J Mech Sci 2013;68:199–211. doi:10.1016/j.ijmecsci.2013.01.016.

[7] Naebe M, Shirvanimoghaddam K. Functionally graded materials: A review of fabrication and properties. Appl Mater Today 2016;5:223–45. doi:10.1016/j.apmt.2016.10.001.

[8] Chen WW. Experimental Methods for Characterizing Dynamic Response of Soft

Materials. J Dyn Behav Mater n.d.;2. doi:10.1007/s40870-016-0047-5.

[9] Zhao H. TEST METHOD Testing of Polymeric Foams at High and Medium Strain Rates. Polym Test 1997;16:507–16.

[10] Liu J, Saletti D, Pattofatto S, Zhao H. Impact testing of polymeric foam using Hopkinson bars and digital image analysis 2014. doi:10.1016/j.polymertesting.2014.03.014.

[11] Othman R, Aloui S, Poitou A. Identification of non-homogeneous stress fields in dynamic experiments with a non-parametric method. Polym Test 2010;29:616–23. doi:10.1016/J.POLYMERTESTING.2010.03.013.

[12] Chen W, Lu F, Cheng M. Tension and compression tests of two polymers under quasi-static and dynamic loading. Polym Test 2002;21:113–21. doi:10.1016/S0142-9418(01)00055-1.

[13] Hu LL, Yu TX. Dynamic crushing strength of hexagonal honeycombs. Int J Impact Eng 2009;37:467–74. doi:10.1016/j.ijimpeng.2009.12.001.

[14] Kiernan S, Cui L, Gilchrist MD. Propagation of a stress wave through a virtual functionally graded foam. Int J Non Linear Mech 2009;44:456–68. doi:10.1016/j.ijnonlinmec.2009.02.006.

[15] Gupta N. A functionally graded syntactic foam material for high energy absorption under compression 2006. doi:10.1016/j.matlet.2006.06.033.

[16] Gupta N, Ricci W. Comparison of compressive properties of layered syntactic foams having gradient in microballoon volume fraction and wall thickness. Mater Sci Eng A 2006;427:331–42. doi:10.1016/j.msea.2006.04.078.

[17] Zheng J, Qin Q, Wang TJ. Impact plastic crushing and design of density-graded

cellular materials. Mech Mater 2015;94:66–78. doi:10.1016/j.mechmat.2015.11.014.

[18] Koohbor B, Kidane A. Design optimization of continuously and discretely graded foam materials for efficient energy absorption 2016. doi:10.1016/j.matdes.2016.04.031.

[19] Chen W, Lu F, Winfree N. High-strain-rate compressive behavior of a rigid polyurethane foam with various densities. Exp Mech 2002;42:65–73. doi:10.1177/0018512002042001791.

[20] Weißenborn O, Ebert C, Gude M. Modelling of the strain rate dependent deformation behaviour of rigid polyurethane foams 2016. doi:10.1016/j.polymertesting.2016.07.007.

[21] Ravindran S, Koohbor B, Malchow P, Kidane A. Experimental characterization of compaction wave propagation in cellular polymers. Int J Solids Struct 2018;139–140:270–82. doi:10.1016/j.ijsolstr.2018.02.003.

[22] Gibson LJ, Ashby MF. Cellular Solids. Cambridge: Cambridge University Press; 1997. doi:10.1017/CBO9781139878326.

[23] Koohbor B, Ravindran S, Kidane A. Impact Response of Density Graded Cellular Polymers. Dyn. Behav. Mater. Vol. 1, Springer; 2018, p. 17–23.

[24] Zeng HB, Pattofatto S, Zhao H, Girard Y, Fascio V. Impact behaviour of hollow sphere agglomerates with density gradient 2009. doi:10.1016/j.ijmecsci.2009.11.012.